

# OBSERVATIONS OF THE STRUCTURAL CHANGES CAUSED DURING THE REPEATED BENDING FATIGUE TEST OF A 18-8 STAINLESS STEEL \*

By

TAKESHI HAGA\*\*

## 1. Introduction

In the process of a fatigue fracture, the structure changes within the slip band or micro-crack on the surface of specimen often leads to the fracture.

In this connection, W. A. Wood<sup>(1)</sup> reported that the slip motion plays an important role in the formation of a crack and the propagation or the growth of a crack depends upon a jumping mechanism.

P. J. E. Forsyth,<sup>(2)</sup> on the other hand, observed the intrusion and extrusion in the process of fatigue. Then, N. Y. Potakin et al.<sup>(3)</sup> described that a pull-in and pull-out were found out in a slip band of polycrystalline copper at the test under a certain of the stress or strain amplitude.

M. Hempel et al.<sup>(4)</sup> reported that the course and the propagation of a fatigue crack are under control of the different orientations in the crystal grains.

One of the present authors<sup>(5)~(7)</sup> observed already the structural changes caused on the fatigue processes of a aluminum bronze and a carbon steel, and then, researched the differences between the fractographs of the same materials.

In the present study, the origination and the propagation of a crack produced in the 18-8 stainless steel has been studied by optical and electron microscopes. And further, the amplitude changes of bending stress and strain applied to the test specimen were measured and the relation between these amplitude changes and the propagation changes crack was studied.

## 2. Samply and experimental method

### 2. 1. Test sample

Chemical composition of the test material is shown in **Table 1**. The material was prepared into the tensile test specimen shown in **Fig. 1**. It was quenched in water after keeping at 1100°C for one hour. The specimen was then polished with emery

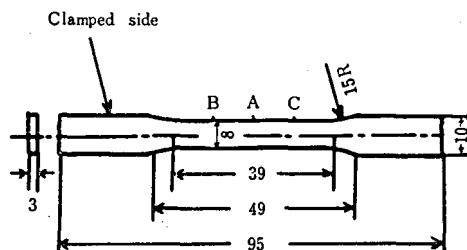
---

\* Proceedings of the 16th Japan Congress on Materials Research 168 (1973)

\*\* *Department of Mechanical Engineering, Nagano Technical College, Nagano.*

**Table 1** Chemical Composition of Test Material (SUS 27) (wt%)

C	Si	Mn	P	S	Ni	Cr	Mo	Cu
0.06	0.57	1.82	0.002	0.009	8.96	18.27	0.18	0.07

**Fig.1** Shape and Dimensions of fatigue Test Specimen.

paper, followed by buffing. A mixed solution of one part of nitric acid, two parts of hydrochloric acid and three parts of glycerin was used as the etching agent in observing the structure. The grain size of the crystalline material was about 0.1–0.3mm. Mechanical properties of the test specimen are given in **Table 2**.

**Table 2.** Mechanical Properties of Test Material  
at Room Temperature (Quenched from 1100°C for 1 hr. heating)

Tensile Strength (kg/mm <sup>2</sup> )	Elongation (%)	Vickers Hardness (300g)
57	63	170

## 2. 2. Experimental method

Fatigue test was performed by a shenk fatigue testing machine. It was by repeated bending fatigue test with the repeated rotational angle varied between 2° to 4° degree. For detection of the stress, four wire resistance strain gauges were attached on the surface of the torque rod, and also the torque changes were detected by the bridge circuit; the values obtained were approved by the static ones. The amplitude changes of the normal bending stresses caused during the fatigue tests were analyzed by the use of these results. The error in stress measurement was about 3%. For detection of the strain, a wire resistance strain gauge was attached on the central portion of the specimen surface, and also the temperature compensation circuit was constructed. The error in this strain measurement was about  $\pm 2.5\%$ . The surface structural changes caused during the fatigue process were observed by the use of both an optical and an electron microscope (by a positive replica technique) at the several steps of the fatigue process.

## 3. Experimental results and discussion

### 3. 1. Approximate S–N curve

The approximate S-N curve in bending fatigue of the 18-8 stainless steel is given in Fig. 2. Here, three levels of the stress amplitudes are corrected, that is, the low stress amplitude refers to  $\sigma=22\pm1\text{kg/mm}^2$  (the number for a fracture  $N=1\times 10^6$  cycles), the intermediate amplitude to  $\sigma=27\pm2\text{kg/mm}^2$  (the number for a fracture  $N=1\times 10^5$  cycles), and the high amplitude to  $\sigma=32\pm5\text{kg/mm}^2$  (the number for a fracture  $N=7\times 10^4$  cycles). The fatigue strength of the test material (at  $N=1\times 10^7$  cycles) was about  $\sigma=16\text{kg/mm}^2$ .

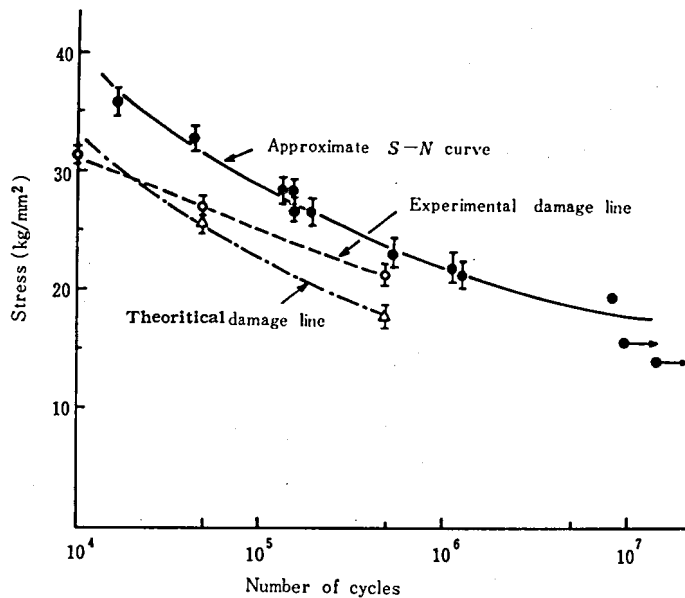


Fig. 2 Relation among Approximate S-N curve, Experimental Damage line and Theoretical Damage line. (The last line was determined from the theory suggested by H. French<sup>10</sup>)

In this paper the approximate S-N curve described is corrected especially by the reason of that the constant stress or strain amplitude can not be kept during the whole fatigue process by the use of the schenk type tester. That is, while the total repeated rotational angle,  $\pm\varphi$ , on the drive side of the tester can be maintained at a constant value, the bending stress applied to the test specimen on the fatigue process is changed by the occurrence of a work hardening or softening. In this case, therefore, the precise S values on the vertical axis of the S-N curve are not established.

This fact is evident as shown in Fig. 3, which shows the relationship between the stress and the number of repeated cycles. In the cases of both the high and the intermediate amplitudes, the strain amplitudes are larger in the beginning of test, but they decrease with increase of the repetitions. The present authors considered that this phenomenon was provably caused by the stress relaxation phenomenon. In the case of the low

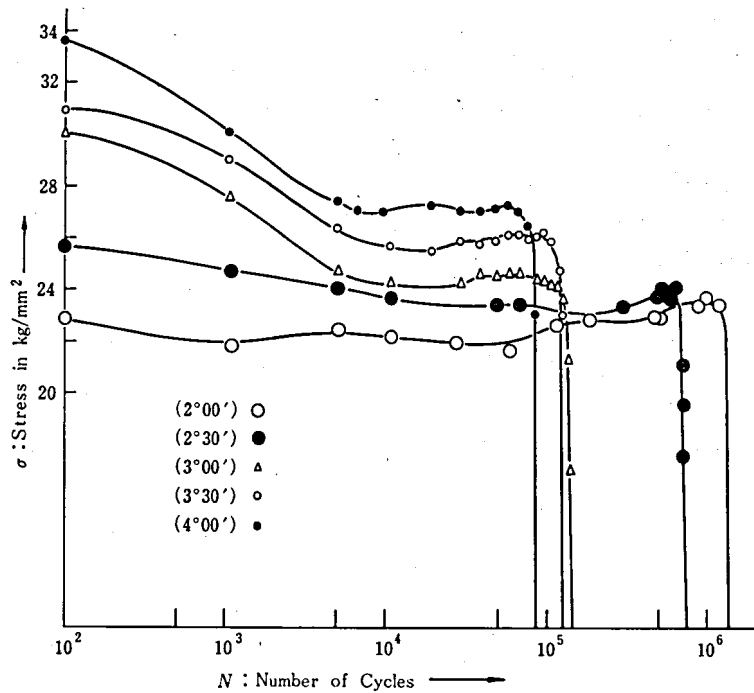


Fig. 3 The Stress Amplitude change taking place during the Fatigue process

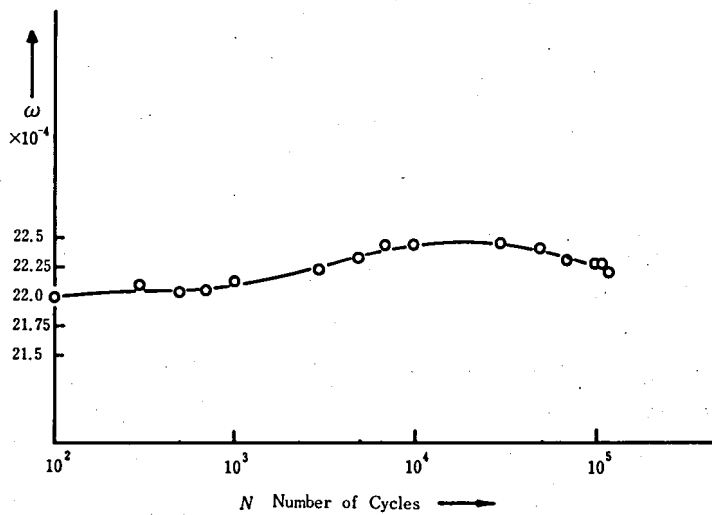


Fig. 4 The Stress Amplitude change caused during the Fatigue Test  
(The repeated rotational angle of 3 degree,  $\sigma = 27 \pm 2 \text{ kg/mm}^2$ )

stress amplitude, the increase and decrease phenomena in stress amplitude caused at about the repetition of  $6 \times 10^5$  were occurred in connection with the multiplication, fixation and

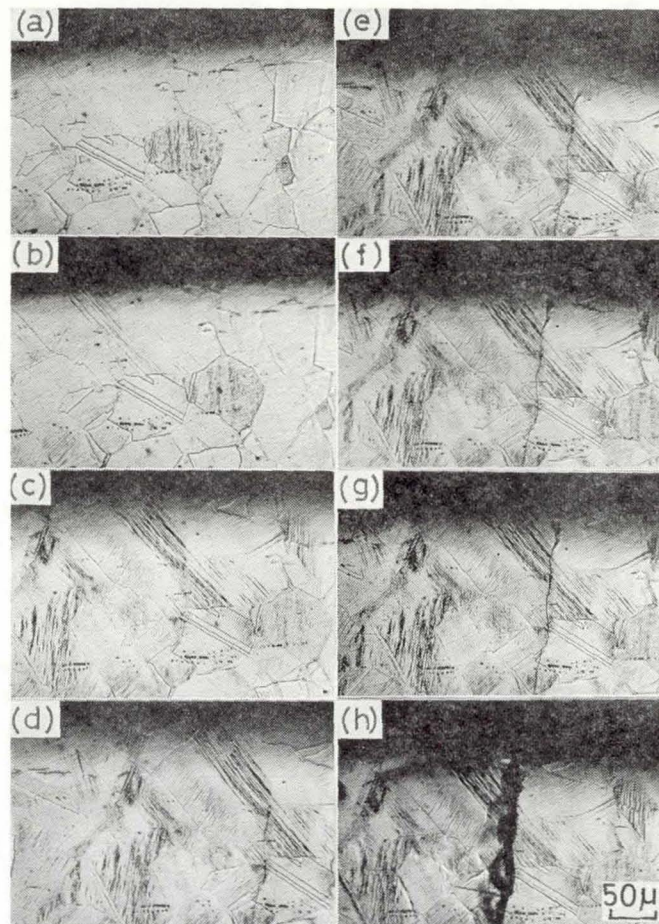
movement of dislocations, or connection with the origination of micro-cracks.

In the case of the intermediate stress amplitude (the rotational angle of  $\pm 3$  degree,) the relations between stress amplitude changes and the number of cycles are shown in Fig. 4.

The results observed here can be explained by the phenomena that the stress amplitude increases gradually with decrease of the strain amplitude, and the strain amplitude takes a maximum value at the repetition which the lowest stress amplitude occurred.

### 3. 2. Observation by the optical microscope

The structural changes caused during the fatigue tests under the three stress levels mentioned above were observed by the optical microscope. These observations are performed concentrically at the three portions, A, B and C on the surface of the test specimen



(a) $N=5 \times 10^3$  (b) $N=1 \times 10^4$  (c) $N=5 \times 10^4$  (d) $N=1 \times 10^5$   
 (e) $N=1.1 \times 10^5$  (f) $N=1.4 \times 10^5$  (g) $N=1.5 \times 10^5$  (h) $N=1.55 \times 10^5$

**Photo. 1** Changes of the structure produced by the repeated bending fatigue test ( $\sigma=27 \pm 2 \text{ kg/mm}^2$ ,  $N=1.55 \times 10^5$ )

as shown in Fig. 1.

**Photo. 1** shows the structural changes caused in the vicinity of the point A on the specimen surface fatigued under the intermediate stress amplitude. Photo. 1 (a) was obtained at a repetition of  $N=5 \times 10^3$ ; a slip band was observed at all A, B and C points. The slip band was uniform, similar to case of the low or high stress amplitude. It was larger in number, however, than the case of the low stress amplitude. The double or transverse slip bands as observed with the high stress amplitude were hardly seen. As in indicated in photo. 1 (b) at  $N=1 \times 10^4$ , the increase in extension of the uniform slip band with the number of cycles is more remarkable than with the low stress amplitude. But, occurrence of other slip band is not observed.

In Photo. 1 (c) obtained at  $N=5 \times 10^4$ , the initial micro-crack (the thick, blackish line of about 1~2mm in length, in 200 magnifications) is caused along the grain boundary or the slip band in perpendicular to the longitudinal direction of the specimen, in the vicinity of the periphery of the specimen. The slip bands in the vicinity of this microcrack include probably the sub-microcracks, as indicated by the black-colored corrosion.

The slip band occurring in crystal grains at  $N=1 \times 10^4$  cycles are retained with increase in the number of cycles, as in the case of the low or the high stress amplitude.

In Photo. 1 (d) obtained at  $N=1 \times 10^5$ , the sub-microcrack produced at  $N=5 \times 10^4$  cycles grows into new form, traversing the slip band in a crystal grain. As seen in photo. 1 (e), (f) and (g), the crack grows with increase of the cycles and at last, arrives at the another edge of the specimen in perpendicular to its longitudinal axis.

In Photo. 1 (h) obtained at  $N=1.55 \times 10^5$  cycles, a fracture occurs in the specimen, mainly along the grain boundary. The slip band in a crystal grain then develops into a crack when its orientation coincides with that of a grain boundary.

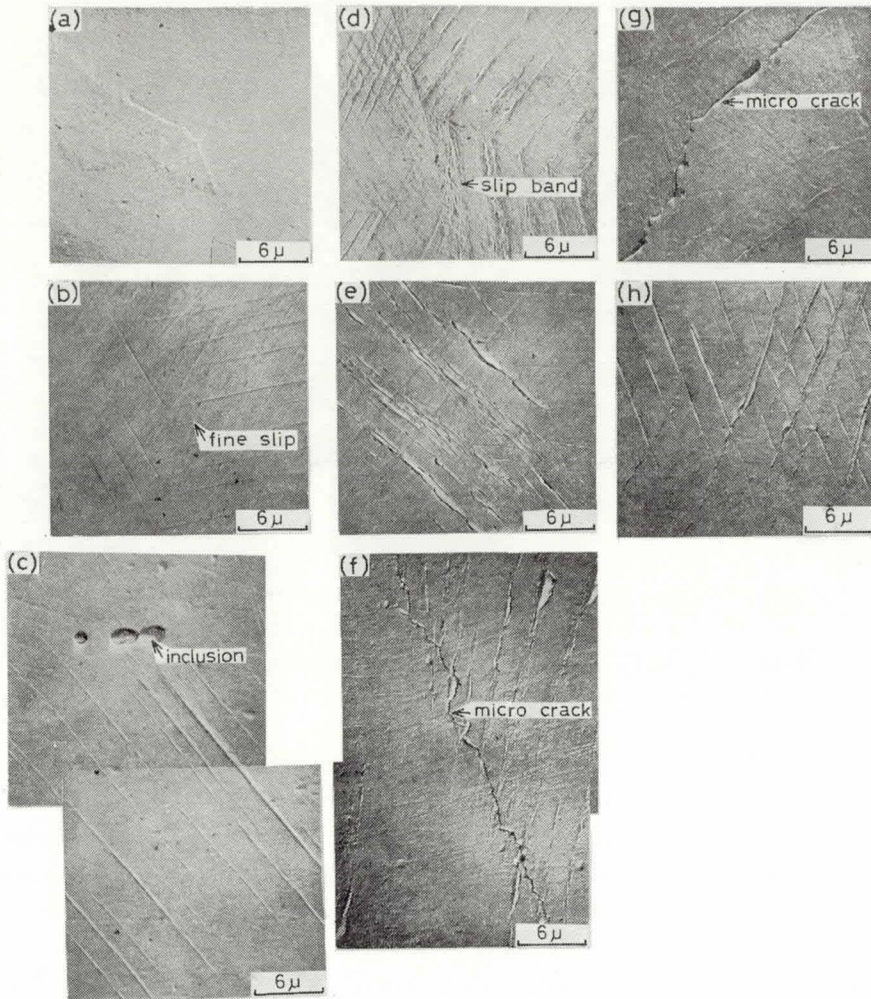
This result is in good agreement with that reported by P.C. Boettner et al.<sup>(8)(9)</sup> that is, the grain boundary gives rise to a minute crack, which then develops into a large one by growth.

### 3. 3. Observation of the structure changes by the use of the Electron Microscope MICROSCOPE

**Photo. 2** shows the structural changes observed by the electron microscope in the vicinity of point A of the specimen in the case of the intermediate stress amplitude, corresponding to those in photo. 1 obtained by an optical microscope.

Photo. 2 (a) shows the surface of the virgin specimen. Photo. 2 (b) was obtained at the repetitions of  $N=5 \times 10^3$ . In this photograph, the slips are in the uniform distributed state, and equivalent to the results obtained from the observation by the optical microscope and they are also observed at the tests of the low and high stress amplitudes. The rippling slip line, as seen on the non-oxidized copper or aluminum bronze specimens, is not observed. With increase of the cycles, each slip line broadens as shown in Photo. 2 (c) obtained at  $N=1 \times 10^4$ . And then, there occur small intrusions or extrusions of





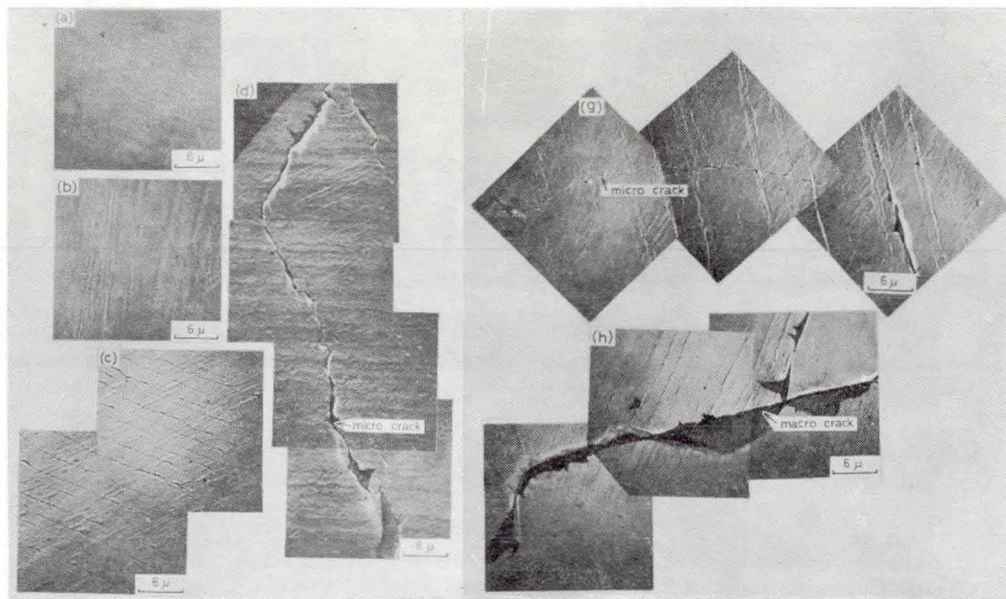
(a)  $N=0$  (b)  $N=5 \times 10^3$  (c)  $N=1 \times 10^4$  (d)  $N=5 \times 10^4$

(e)  $N=1 \times 10^5$  (f)  $N=1.2 \times 10^5$  (g)  $N=1.4 \times 10^5$  (h)  $N=1.55 \times 10^5$

**Photo. 2** Changes the structure produced by the intermediate stress amplitude fatigue test. ( $\sigma=27 \pm 2 \text{ Kg/mm}^2$ ,  $N=1.55 \times 10^5$ )

about  $0.05\mu$  in depth along the slip line as shown in Photo. 2 (d) obtained at  $N=5 \times 10^4$  cycles. They grow into the remarkable ones of about  $0.3 \sim 1.0\mu$ , with further increase of the cycles. These intrusions and extrusions are the double or transverse slips observed in the grains, and in the particular case, the larger ones are observed along the grain boundaries.

Photo. 2 (e) shows a structure at  $N=1 \times 10^5$  cycles. The sub-microcracks are observed



(a)  $N = 5 \times 10^2$  (b)  $N = 1 \times 10^3$  (c)  $N = 5 \times 10^3$   
 (d)  $N = 3 \times 10^4$  (g)  $N = 7.3 \times 10^4$  (h)  $N = 7.43 \times 10^4$

**Photo. 3** changes of the Structure produced by the high stress amplitude fatigue test. ( $\sigma = 32 \pm 5 \text{ kg/mm}^2$ ,  $N = 7.43 \times 10^4$ )

at the same portion in Photo. 1 (d) obtained by the optical microscope and they are found out as the small intrusions and extrusions. The present authors considered that the intrusions or extrusions with depth or height about  $2 \sim 4 \mu$  are to be the microcracks and then, they with depth over about  $4 \mu$  are to be the macrocracks. The intrusions along the slip lines in the vicinity of the microcracks are about  $0.2$  and they are the sub-microcracks.

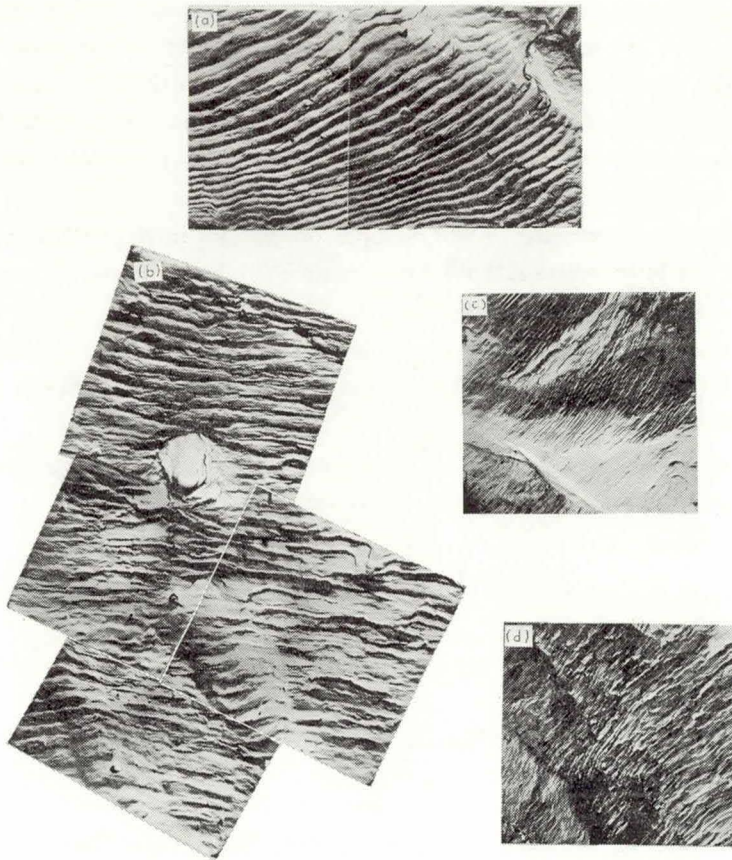
In Photo. 2 (f) and (g) obtained at  $N = 1.2 \times 10^5$  and  $N = 1.4 \times 10^5$  cycles, the authors confirmed that the propagation of microcrack was restricted by the orientations in the austenitic phase and depended upon the jumping mechanism suggested by W. A. wood.<sup>1</sup>

Photo. 2 (h) shows the feature of a crossing intrusions observed in the vicinity of the fracture line on the surface of the specimen, this specimen fractured at the repetitions of  $N = 1.554 \times 10^5$ .

The occurrences and developments of the structural changes conform to the following course, that is, from the uniform fine slip to the slip band, then to the intrusion or the extrusion, to the micro-crack, to the macro-crack and finally to the fracture.

In the case of the low and the high stress amplitudes tests, the occurrence and the development of the structural changes were generally similar to those for the intermediate stress amplitude, but especially, it was found out that the propagations of a micro-crack and macro-crack were not restricted by the slip systems in of the austenitic phases of





**Photo. 4** Fracture Surface produced by the Intermediate stress Amplitude Fatigue Test ( $\sigma = 27 \pm 2 \text{ kg/mm}^2$ )

a specimen under the test of the high stress amplitude. An evidence for them are presented in **Photo. 3**.

Four fractographs corrected from the several portions on the fracture surface produced by the fatigue test under the stress amplitude of  $\sigma = 27 \pm 2 \text{ kg/mm}^2$  are presented in **Photo. 4**. Photo. 4 (a), (c) and (d) show the disturbance of the striation modes caused by the grain boundary, and the change of striation modes produced by a inclusion is presented in Photo. 4 (b).

#### 4. Conclusion

(1) Using a Schenk type fatigue testing machine, the true S-N curve is notable to be obtained. This because that the stress amplitude is a variable quantity as shown in Fig. 3. The curve in this case is thus to be called the "approximate" S-N curve.

(2) The changes in amplitudes of the stress and strain are in close connection with the structural changes.

(3) The occurrences and developments of the structural changes conform to following course, that is, from the uniform fine slip to the slip band, then to the intrusion or the extrusion, to the micro-crack, to the macro-crack and finally to the fracture.

(4) The occurrence of a micro-crack was observed at the corner part of a grain boundary which situated about 0.2-0.3mm distance from the periphery of the central portion of the specimen surface.

Its propagation was restricted by the multiple orientations in the austenitic phase in by the cases of the intermediate and the low stress amplitudes, but was not restricted in the case of the high amplitude test.

(5) The grain boundary or the inclusion has the effect of preventing the propagation of the several kinds of the structural changes and the extension of the crack.

#### ACKNOWLEDGEMENT

The authors are indebted to Mr. C. Minamisawa of Defence Academy for his encouragement, and to Mr. Aoki and Mr. Ishida for their assistance.

#### References

- (1) W. A. Wood, e.g., *Phil. Mag.*, **3**, 692 (1958)
- (2) P. J. E. Forsth, *Inst. Metals*, **82**, 449 (1953-54)
- (3) N. Ye. Potakhin and Yu. S. Terminasov, *Phys. Met. and Metallog.*, **16**, No. 1, 86 (1963)
- (4) F. Werer, M. Hempel und A. Schrader, e. g., *Archiv Eisenhuttenw*, **26**, 739 (1955)
- (5) T. Haga, e. g., *Jr. of SMS*, **18-188**, 405 (1969)
- (6) T. Haga, *Jr. of SMS*, **19-197**, 90 (1970)
- (7) C. Minamisawa, M. Sekikawa and T. Haga, *Proc. 15th. Japan Conr. on Materials Research*, **22** (1972)
- (8) R. C. Boettner, C. Laird, and A. J. McEvily, Jr., *Trans. AIME*, **233**, 379 (1965)
- (9) R. C. Boettner, *Trans. AIME*, **239**, 1030 (1967)
- (10) H. French, *Trans. ASTM*, **21**, 899 (1933)